

REPORT DOCUMENTATION PAGE			Form Approved OMB NO. 0704-0188		
<p>The public reporting burden for this collection of information is estimated to average 1 hour per response, including the time for reviewing instructions, searching existing data sources, gathering and maintaining the data needed, and completing and reviewing the collection of information. Send comments regarding this burden estimate or any other aspect of this collection of information, including suggestions for reducing this burden, to Washington Headquarters Services, Directorate for Information Operations and Reports, 1215 Jefferson Davis Highway, Suite 1204, Arlington VA, 22202-4302. Respondents should be aware that notwithstanding any other provision of law, no person shall be subject to any penalty for failing to comply with a collection of information if it does not display a currently valid OMB control number.</p> <p>PLEASE DO NOT RETURN YOUR FORM TO THE ABOVE ADDRESS.</p>					
1. REPORT DATE (DD-MM-YYYY) 20-12-2007		2. REPORT TYPE Final Report		3. DATES COVERED (From - To) 25-Sep-2003 - 24-Sep-2007	
4. TITLE AND SUBTITLE Plasma-Propellant Interaction Studies			5a. CONTRACT NUMBER DAAD19-03-1-0340		
			5b. GRANT NUMBER		
			5c. PROGRAM ELEMENT NUMBER 611102		
6. AUTHORS Stefan T. Thynell, Thomas A. Litzinger			5d. PROJECT NUMBER		
			5e. TASK NUMBER		
			5f. WORK UNIT NUMBER		
7. PERFORMING ORGANIZATION NAMES AND ADDRESSES Pennsylvania State University Office of Sponsored Programs The Pennsylvania State University University Park, PA 16802 -			8. PERFORMING ORGANIZATION REPORT NUMBER		
9. SPONSORING/MONITORING AGENCY NAME(S) AND ADDRESS(ES) U.S. Army Research Office P.O. Box 12211 Research Triangle Park, NC 27709-2211			10. SPONSOR/MONITOR'S ACRONYM(S) ARO		
			11. SPONSOR/MONITOR'S REPORT NUMBER(S) 45452-EG.4		
12. DISTRIBUTION AVAILABILITY STATEMENT Approved for Public Release; Distribution Unlimited					
13. SUPPLEMENTARY NOTES The views, opinions and/or findings contained in this report are those of the author(s) and should not be construed as an official Department of the Army position, policy or decision, unless so designated by other documentation.					
14. ABSTRACT This report describes research focused on the interactions between a plasma and a solid propellant. The specific issues addressed include the effects of radical and neutral species as well as radiative heat transfer on the ignition and combustion of double-base propellants. A wide variety of measurements have been conducted using a broad range of diagnostic tools, such as a triple-quadrupole mass spectrometer, special heat flux gages, high-speed cameras, as well as SEM and X-ray facilities. Species measurements show that both neutrals/radicals and ions from the capillary arrive at the propellant surface and provide a pool of species that readily interact with pyrolysis products from the propellant. It is also evident that metal					
15. SUBJECT TERMS Plasma, propellant, mass spectrometry, radiative heat transfer, ions, capillary					
16. SECURITY CLASSIFICATION OF:		17. LIMITATION OF ABSTRACT		15. NUMBER OF PAGES	19a. NAME OF RESPONSIBLE PERSON
a. REPORT U	b. ABSTRACT U	c. THIS PAGE U	SAR		Stefan Thynell
					19b. TELEPHONE NUMBER 814-865-1345

Report Title

Plasma-Propellant Interaction Studies

ABSTRACT

This report describes research focused on the interactions between a plasma and a solid propellant. The specific issues addressed include the effects of radical and neutral species as well as radiative heat transfer on the ignition and combustion of double-base propellants. A wide variety of measurements have been conducted using a broad range of diagnostic tools, such as a triple-quadrupole mass spectrometer, special heat flux gages, high-speed cameras, as well as SEM and X-ray facilities. Species measurements show that both neutrals/radicals and ions from the capillary arrive at the propellant surface and provide a pool of species that readily interact with pyrolysis products from the propellant. It is also evident that metal particles from trigger wire and nozzle arrive at the propellant surface to enhance the pyrolysis. The magnitudes of the radiative heat transfer are extremely high and depend on the capillary and trigger wire material used. The radiation produces measurable pyrolysis and in-depth heating of transparent JA2. The ultra-violet component is very strong, but it is believed to inhibit ignition when the propellant is directly exposed to the plasma. The pyrolysis species, including NO₂, N₂O, HONO and aldehydes are uv-photolyzed, to produce CO, CO₂, NO and CH₄.

List of papers submitted or published that acknowledge ARO support during this reporting period. List the papers, including journal references, in the following categories:

(a) Papers published in peer-reviewed journals (N/A for none)

Interaction of capillary plasma with double-base and composite propellants, Li, Jianquan; Litzinger, Thomas A.; Thynell, Stefan T. Journal of Propulsion and Power, v 20, n 4, 2004, pp. 675-683.

Plasma ignition and combustion of JA2 propellant, Li, Jianquan; Litzinger, Thomas A.; Thynell, Stefan T. Journal of Propulsion and Power, v 21, n 1 2005, pp. 44-53.

Study of plasma-propellant interaction during normal impingement, Li, Jianquan; Litzinger, Thomas A.; Das, Malay; Thynell, Stefan T., Journal of Propulsion and Power, v 22, n 5, 2006, pp. 929-937.

Recombination of electrothermal plasma and decomposition of plasma-exposed propellants, Li, Jianquan; Litzinger, Thomas A.; Das, Malay; Thynell, Stefan T., Journal of Propulsion and Power, v 22, n 6, 2006, pp. 1353-1361.

Das, M., Thynell, S. T., Li, J-Q., and Litzinger, T, "Transient radiative Heat Transfer From a Plasma Produced by a Capillary Discharge", Journal of Thermophysics and Heat Transfer, Vol. 19, No. 4, 2005, pp. 572-580.

Das, M., Thynell, S. T., Li, J-Q., and Litzinger, T, "Material Dependence of Plasma Radiation Produced by a Capillary Discharge", Journal of Thermophysics and Heat Transfer, Vol. 20, No. 3, 2005, 595-603.

Das, M., and Thynell, S. T., "Two-dimensional Conduction Effect in Estimating Radiative Heat Flux from a Capillary Discharge", Journal of Thermophysics and Heat Transfer, Vol. 20, No. 4, 2006, pp. 903-911.

Number of Papers published in peer-reviewed journals: 7.00

(b) Papers published in non-peer-reviewed journals or in conference proceedings (N/A for none)

Number of Papers published in non peer-reviewed journals: 0.00

(c) Presentations

Number of Presentations: 0.00

Non Peer-Reviewed Conference Proceeding publications (other than abstracts):

Das, M., Thynell, S. T., Li, J-Q., and Litzinger, T, "Transient radiative Heat Transfer From a Plasma Produced by a Capillary Discharge", Proceedings of 40th Jannaf Combustion Meeting, Charleston, South Carolina, June 13-17, 2005.

Das, M., Thynell, S. T., Li, J-Q., and Litzinger, T, "Material Dependence of Plasma Radiation Produced by a Capillary Discharge", Proceedings of 40th Jannaf Combustion Meeting, Charleston, South Carolina, June 13-17, 2005.

Li, J-Q., Litzinger, T, Das, M., and Thynell, S. T., "Normal Impingement of Electrothermal Plasma on Solid Propellant", Proceedings of 40th Jannaf Combustion Meeting, Charleston, South Carolina, June 13-17, 2005.

Number of Non Peer-Reviewed Conference Proceeding publications (other than abstracts): 0

Peer-Reviewed Conference Proceeding publications (other than abstracts):

Li, J-Q., Litzinger, T, Das, M., and Thynell, S. T., "Species Measurement during ETC Plasma Recombination and its interaction with Propellants", Proceedings of 41st AIAA/ASME/SAE/ASEE Joint Propulsion Conference and Exhibit, Tucson, Arizona, July 10-13, 2005.

Das, M., Thynell, S. T., Li, J-Q., and Litzinger, T, "Material Dependence of Capillary-Sustained Plasma Radiation", 9nd AIAA/ASME Joint Thermophysics and Heat Transfer Conference, San Francisco, California, June 5-8, 2006.

Das, M., and Thynell, S. T., "Two-dimensional Conduction Effect in Estimating Radiative Heat Flux from a Plasma Jet", 9nd AIAA/ASME Joint Thermophysics and Heat Transfer Conference, San Francisco, California, June 5-8, 2006.

Das, M K., Chowdhury A., and Thynell, S T., "Radiative Pyrolysis of JA2 from an Electrochemical Plasma Discharge", 2007 Fall Technical Meeting, Eastern State Section of the Combustion Institute, University of Virginia, Oct 21 – 24, 2007.

Number of Peer-Reviewed Conference Proceeding publications (other than abstracts): 4

(d) Manuscripts

Number of Manuscripts: 0.00

Number of Inventions:

Graduate Students

<u>NAME</u>	<u>PERCENT SUPPORTED</u>
Jianquan Li	0.50
Malay Das	0.50
FTE Equivalent:	1.00
Total Number:	2

Names of Post Doctorates

<u>NAME</u>	<u>PERCENT SUPPORTED</u>
Jianquan Li	0.50
Suresh Iyer	0.10
FTE Equivalent:	0.60
Total Number:	2

Names of Faculty Supported

<u>NAME</u>	<u>PERCENT SUPPORTED</u>	National Academy Member
Stefan Thynell	0.03	No
Thomas Litzinger	0.03	No
FTE Equivalent:	0.06	
Total Number:	2	

Names of Under Graduate students supported

<u>NAME</u>	<u>PERCENT SUPPORTED</u>
Jason Volpe	0.00
FTE Equivalent:	0.00
Total Number:	1

Student Metrics

This section only applies to graduating undergraduates supported by this agreement in this reporting period

The number of undergraduates funded by this agreement who graduated during this period:	0.00
The number of undergraduates funded by this agreement who graduated during this period with a degree in science, mathematics, engineering, or technology fields:.....	0.00
The number of undergraduates funded by your agreement who graduated during this period and will continue to pursue a graduate or Ph.D. degree in science, mathematics, engineering, or technology fields:.....	0.00
Number of graduating undergraduates who achieved a 3.5 GPA to 4.0 (4.0 max scale):.....	0.00
Number of graduating undergraduates funded by a DoD funded Center of Excellence grant for Education, Research and Engineering:.....	0.00
The number of undergraduates funded by your agreement who graduated during this period and intend to work for the Department of Defense	0.00
The number of undergraduates funded by your agreement who graduated during this period and will receive scholarships or fellowships for further studies in science, mathematics, engineering or technology fields:	0.00

Names of Personnel receiving masters degrees

<u>NAME</u>
Total Number:

Names of personnel receiving PHDs

<u>NAME</u>	
Jianquan Li	
Malay Das (Spring 2008)	
Total Number:	2

Names of other research staff

<u>NAME</u>	<u>PERCENT SUPPORTED</u>
Larry Horner	0.05 No
FTE Equivalent:	0.05
Total Number:	1

Sub Contractors (DD882)

Inventions (DD882)

Plasma-Propellant Interaction Studies

Final Report to Project Fund Number DAAD19-03-1-0340, P-45452-EG

Stefan T. Thynell and Thomas A. Litzinger
Department of Mechanical and Nuclear Engineering
The Pennsylvania State University
University Park, PA 16802

TABLE OF CONTENTS.....	1
STATEMENT OF THE PROBLEM STUDIED.....	2
SUMMARY OF MOST IMPORTANT FINDINGS.....	2
Species from Plasma Measurements.....	2
Species from Plasma-Propellant Interactions.....	8
Radiative Heat Transfer Measurements from Plasma.....	11
Radiative Ignition of Double-Base Propellants.....	16
Technology Transfer.....	18
References.....	18

STATEMENT OF THE PROBLEM STUDIED

The use of a high-temperature and high-pressure plasma for ignition of solid propellants has recently received considerable attention.¹⁻⁸ The use of a plasma has revealed a burn-rate enhancement during the electrical discharge process, but it is not clear why this enhancement occurs. The high temperatures and pressures produce a complex interaction between the plasma and the propellant, as well as it involves several modes of energy transport. First, the characteristic velocities and thermal conductivity of the plasma are large, thereby producing high convective heat transfer coefficients. Second, the plasma contains electrons, ions, atoms and low molecular-weight species from the ablation of capillary and electrodes that contribute significantly to the thermal radiation in the UV-visible wavelength range. Third, as the plasma cools, in particular in the interaction region near the propellant's surface, heat is released from recombination reactions among electrons, ions, atoms and low molecular-weight species. Finally, chemical reactions between products from the solid propellant and products from the plasma may enhance the chemical reactions, thereby producing reduced ignition delays compared to conventional ignition systems. However, few studies are available in the literature that have attempted to identify species that arrive and interact with the pyrolysis products of the propellant, and the magnitudes of the transient radiative heat transfer rates from plasmas generated by capillary discharges are largely unknown.

Two experimental approaches were applied. A triple-quadrupole mass spectrometer was employed to examine species from the plasma and the pyrolysis products from the propellant generated by interactions with the plasma. A fast-response heat flux gauge was designed and utilized to determine the transient variation of the radiant heat flux, with specific emphasis on the UV to near-visible components. Other diagnostic tools were also used, including pressure transducers, current transducers, and high-speed cameras, as well as SEM and X-ray facilities. Results show that neutrals and ions from the plasma are present near the propellant surface, and thus likely participants in enhancement of ignition and combustion. Results also show that the radiative heat flux levels are extraordinarily high, but uv-photolysis is likely to have an adverse effect on ignition and combustion.

SUMMARY OF MOST IMPORTANT FINDINGS

Species from Plasma Measurements

One of the potentially important interactions during a plasma-propellant ignition event is that of the highly reactive plasma species reacting with the propellant itself and gas-phase products from propellant decomposition. To determine what reactive species are present in the plasma, a series of experiments were conducted to investigate the composition of the plasma using molecular beam sampling and mass spectrometric analysis. The key experimental variables were the amount of energy input to the plasma generator and the type of capillary material, in this case polyethylene and Lexan. Limited testing was also done with Teflon.

The overall experimental set-up for these studies is presented in Fig. 1. The pulse forming network is based on a resistance-inductance-capacitor circuit, which is mainly composed of an energy storage component that consists of two high-voltage fast-

discharge capacitors connected in parallel to yield a total capacitance of 192 μF , pulse-shaping components including a 20 μH inductor and a crowbar diode, and a floating high-voltage mercury switch (ignitron) as the trigger unit. The capacitors can be charged up to 10 kV corresponding to maximum energy storage of 9.6 kJ. The plasma chamber consists of a capillary liner, a fine metallic wire, electrodes, and other conducting or non-conducting housing hardware. The electrodes are made of erosion-resistant material, elkonite, a copper-tungsten alloy (30% Cu, 70% W). Inside the capillary is a fine copper filament (0.08 mm) connecting the electrodes and serving as the discharge initiator. After being formed immediately upon triggering the ignitron, the generated plasma flows through a nozzle that has typical dimensions of 3.2 mm [inner diameter (ID)] and 13.5 mm (length) into open air or a closed chamber.

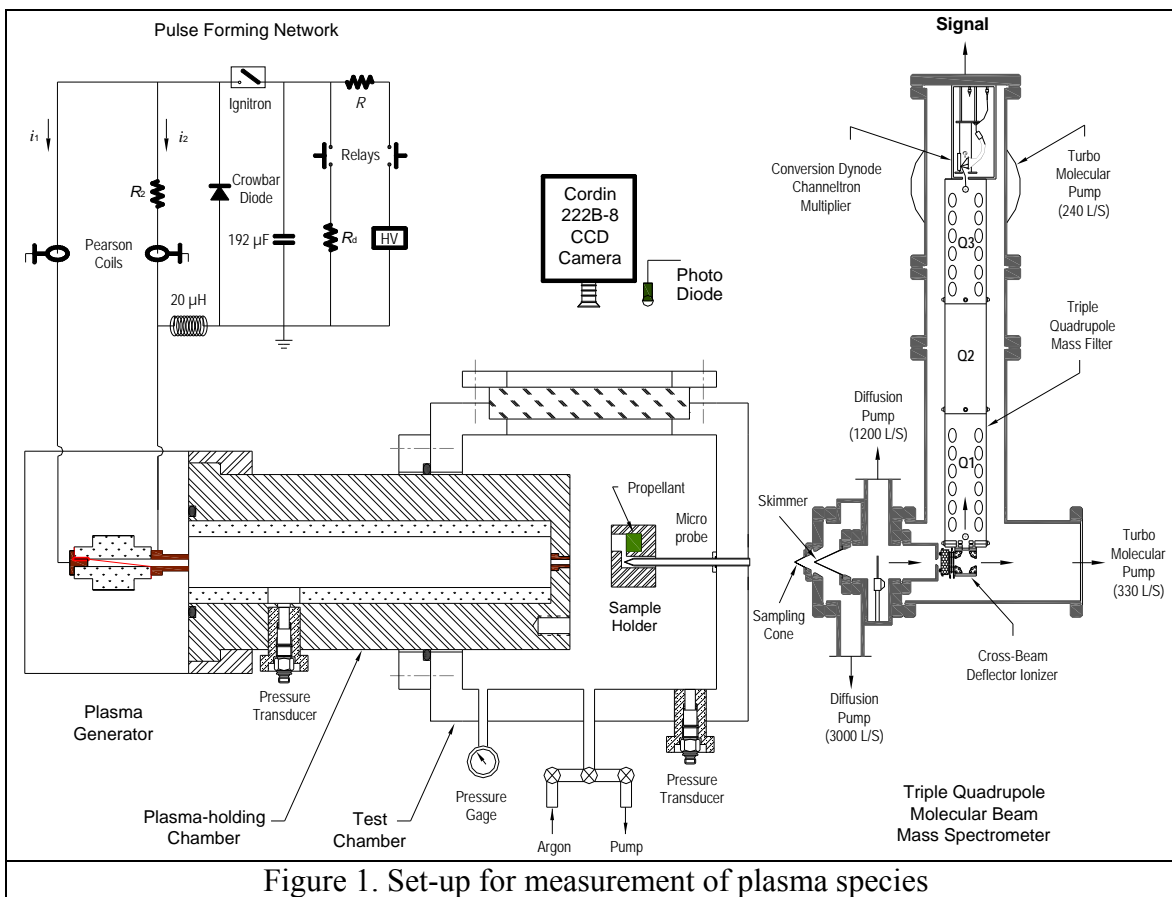


Figure 1. Set-up for measurement of plasma species

The mass spectrometer, also depicted in Fig. 1, is an Extrel triple-quadrupole mass spectrometer (TQMS) with two sampling schemes: one using tubular microprobes and the other using a cone skimmer configuration. In microprobe sampling, two quartz probes are usually used. The primary probe has dimensions of 50 mm (length), 2 mm (ID) and 3.2 mm [outer diameter (OD)]; its front end is fabricated by pulling during torch heating to form a conical tip, which is then ground to open an orifice of about 50 μm in diameter. The secondary probe (not shown in the figure) is 120 mm (length), 4 mm (ID) and 6.35 mm (OD). The orifice of the secondary probe is about 100 μm , which is placed behind the primary probe with a gap of ~ 1.0 mm. The advantages of the microprobe sampling

are better spatial resolution and larger strength to take higher pressures in the test chamber. In the cone-skimmer scheme, a cone-shaped sampler is used, which is 20 mm long and has an orifice of 100 μm at its apex. The selection of relatively large included angles (interior 50 deg and exterior 55 deg) is expected to allow a “free” expansion for the supersonic jet developing inside. The skimmer is comparatively large both in length (50 mm) and in orifice diameter (1.5 mm), and has a 55 deg interior angle and a 60 deg exterior angle. The use of cone-skimmer scheme enables molecular beam sampling to directly probe unstable intermediate species such as radicals and ions, which is desirable for applications like plasma species measurements. The ionizer is an Extrel cross-beam-deflector ionizer, which is a combination of an axial ionizer mounted perpendicularly to the mass filter axis and a small quadrupole deflector energy filter.

Initial efforts in plasma species measurements were made to directly probe the species of plasma jets during freely expanding in open air. However, it was soon found that the temporal mismatch between the plasma pulse of less than 0.3 ms and the requirement for sampling duration by the mass spectrometer, ~ 1 ms, made direct sampling from the jet practically impossible. Furthermore, the presence of metallic particles in the plasma jet renders difficulty in protecting the sampler orifice from enlargement or even damage, which is especially true for the cone-skimmer configuration. To circumvent these difficulties, a plasma-holding chamber is used, as shown in Fig. 1.

The plasma-holding chamber is a small cylindrical chamber with one end attached to the plasma generator and the other extending to a test chamber and interfacing with the sampling probe through a small nozzle of a 1 mm orifice to slow down the flow out of the chamber. Tubular sleeves of different sizes and/or materials can be inserted in the holding chamber to vary its actual volume. The experiments involved the use of metal (aluminum) and nonmetal (PE, Lexan, or Teflon) materials. The test chamber, which interfaces with the mass spectrometer through a flange that holds the primary microprobe or the cone, has a 10 x 10 x 10 cm internal volume and is equipped with a 6.5 cm circular window for photography.

Other supplementary measurements made during the experiments include pressure histories in the holding chamber, images of the secondary jet, and diode signals that monitor the discharge process of the secondary jet. These measurements are an aid in interpreting the species data. The setup for these measurements is also illustrated in Fig. 1.

Key information for those who may do modeling of the results of these experiments is the atomic composition of the plasma. Although the capillary plasma is initiated by vaporization of the exploding wire and sustained by ablation of the capillary wall material, the wire and the capillary are not the only sources for the plasma mass. The total mass of the plasma jet is composed of contributions from several sources, which, in addition to the trigger wire and capillary, also include the end electrode (anode), the nozzle (cathode), and the air that is initially trapped in the capillary. Generally, because the nozzle undergoes intense radiative and convective heating by the plasma flowing through it at high velocities, ablation of its wall material provides a major fraction to the

total plasma mass. As a result, the mass of metallic particles contributes a major part to the total mass of the plasma jet as shown in Fig. 2a. However, by mole fraction, it is the elements (H and C) from the capillary that dominate over all other species as indicated in Fig. 2b. Therefore, the capillary mass loss due to ablation is of great importance to the chemistry of the plasma.

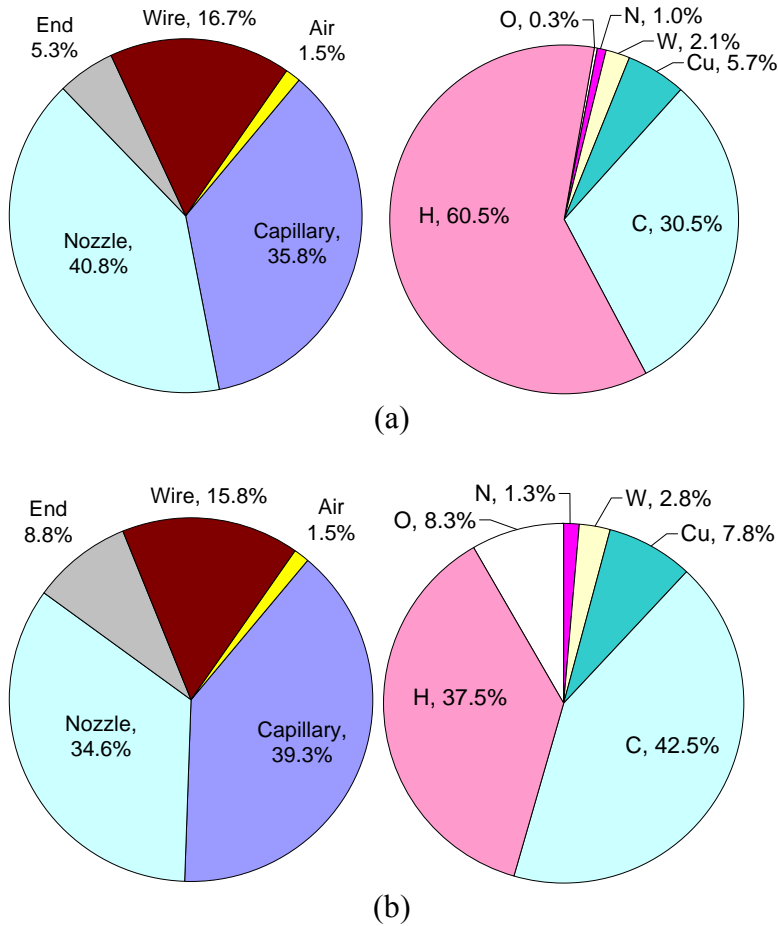


Figure 2. Composition of plasma showing contributions of material from exploding wire and the electrodes

Spectroscopic measurements by Kohel et al. [9] showed that the plasma temperature in the region of upstream of the Mach disk is about 23,400 K at 30 μ s after the pulse discharge begins for a charging voltage at 5 kV. Inside the capillary, the temperature must be even higher. At these temperatures, the plasma is almost completely composed of atomic species, mainly including C, H, C^+ , H^+ and electrons for PE material, and with the addition of O and O^+ for Lexan plasma. After entering the holding chamber, recombination of these atomic species takes place as the temperature drops due to a combination of heat transfer to walls and turbulent mixing with background gases. Heat transfer and mixing will also occur within actual PPI systems, so the processes in the holding chamber approximate those that occur in actual applications.

Sampling of species from the plasma was initially performed through scanning over all possible species resulting from recombination. Variation in test conditions included plasma source material, location of sampling probe in the jet, plasma energy, and initial background conditions. For all conditions considered, the recombined species that could be consistently detected were found to have mass-to-charge ratios (m/z) of 28, 27, 26, 16, 15, 2, and 1 for PE and Lexan. In some tests, species at m/z of 44, 30, and 25 also appeared, but their signals were usually small and they were not consistently detectable. Table 1 presents the major species that are present at each m/z . Differentiation of species that have the same m/z value was enabled through an analysis of daughter ions using MS/MS.

Table 1. Major signals and corresponding species

m/z	44	30	28	27	26	25	16	15	2	1
Ions	CO_2^+	$\text{C}_2\text{H}_6^+/\text{NO}^+$	$\text{C}_2\text{H}_4^+/\text{CO}^+$	C_2H_3^+	C_2H_2^+	C_2H^+	CH_4^+	CH_3^+	H_2^+	H^+
Species	CO_2	$\text{C}_2\text{H}_6/\text{NO}$	$\text{C}_2\text{H}_4/\text{CO}$	C_2H_3	C_2H_2	C_2H	CH_4	CH_3	H_2	H

An important issue was to establish whether the radical species, e.g., H and C_2H_3 , in the plasma were actually present or whether they were products of the electron impact ionization process, even though a rather low energy of 22 eV was being used. Comparison of the fragmentation patterns of key stable species such as C_2H_4 and C_2H_2 showed that radical species were indeed being detected. Details of this study are presented in Ref. 10.

A series of experiments were performed to investigate the effect of input electrical energy on the recombination of plasma for charging voltages ranging from 3 to 6 kV, corresponding to electrical energies of 0.86, 1.56, 2.40, and 3.46 kJ. The plasma chemistry was varied through the use of different materials, PE or Lexan, for the capillary and the holding chamber insert. The typical results from these plasmas are presented in Fig. 3, where the relative intensities of smaller species expressed as ratios over the intensity of $m/z=28$ are plotted against four charging levels of 3, 4, 5, and 6 kV. The intensities for all species considered are averaged over the time period during which the jet issues from the plasma holding chamber.

The data show that an increase in charging voltage increases the relative intensities of smaller species for PE plasma, which is especially true for H_2 (2), CH_3 (15), and CH_4 (16). This trend is an indicator that the plasma energy strongly affects the recombination process, showing that smaller molecules become increasingly dominant in the jet as more energy is deposited into the plasma. The abundance in hydrogen atoms and molecules may be a crucial factor in performance enhancement observed in ETC guns. For Lexan plasma, the energy effect is also evident, and the general trend still applies that higher plasma energies increase the relative intensities of smaller species.

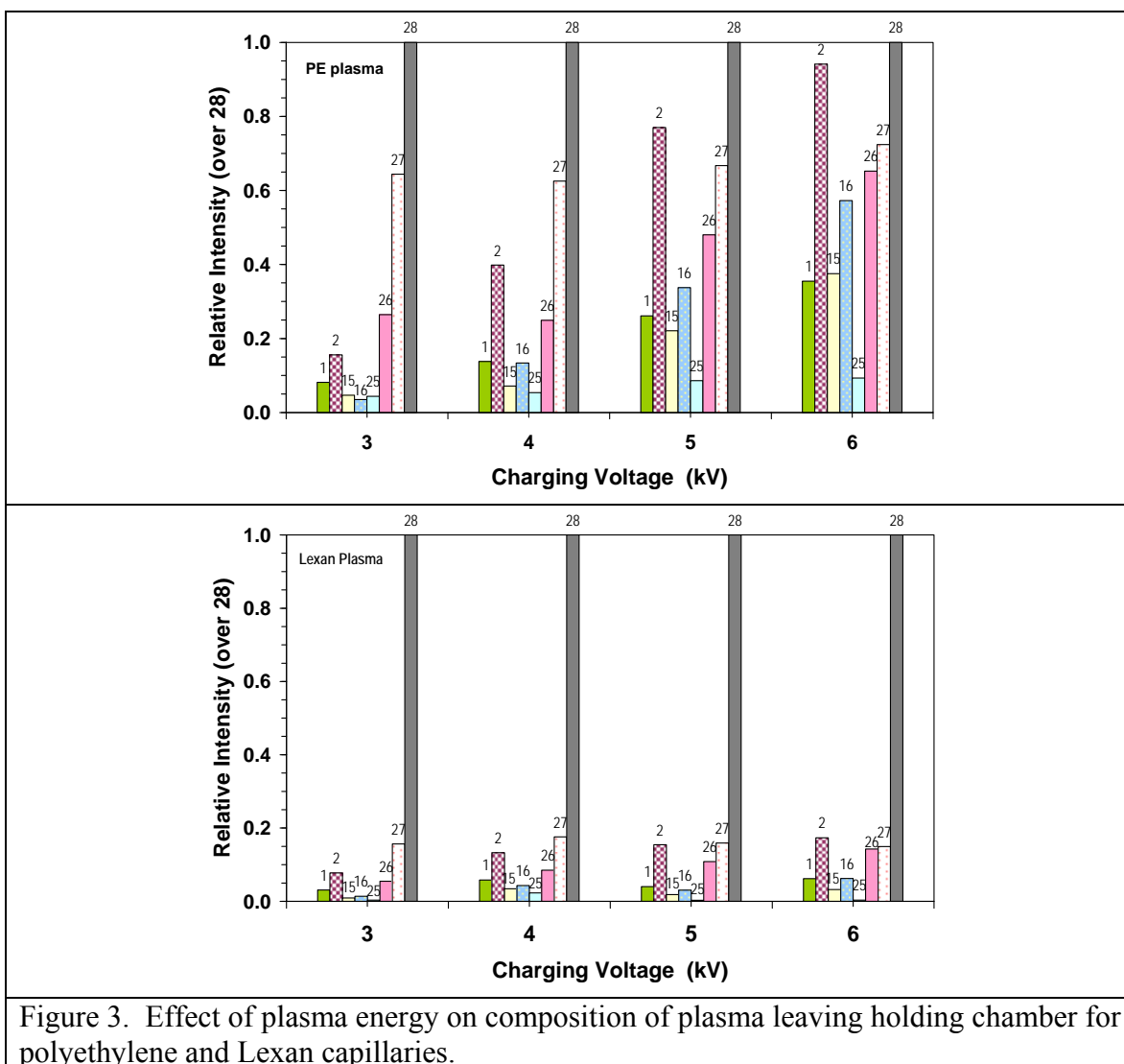


Figure 3. Effect of plasma energy on composition of plasma leaving holding chamber for polyethylene and Lexan capillaries.

Comparing the data for the two materials shows that for the Lexan plasma the relative intensities of species at $m/z = 27$ is significantly lower, and that the species of m/z at 28 dominates over all other species in the jet. This is reasonable given that fact that Lexan ($[C_{16}H_{14}O_3]_n$) contains oxygen and thus has more CO formed in the recombination contributing to mass 28.

Limited testing was done with Teflon capillaries to compare them to the polyethylene results. In these tests, the plasma from a Teflon capillary was fired into the holding chamber, which was lined with Teflon. The species identified were, in a descending order of intensity of signal: C_2H_4 , CO, H_2O , HF, H_2CO , C_2H_6 , NO, CO_2 , CF, F, C_2H_3 , HCN, C_2H_2 , F_2 , H_4C_2F , C_2H , CF_2 , H_2C_2F , CF_3 , COF_2 , H_2 , H_3C_2F , and NO_2 . Figure 4 compares the signals for the Teflon tests and a comparable PE test. The presence of HF and F in the Teflon species may account for the greater mass losses that are observed with Teflon compared to PE.

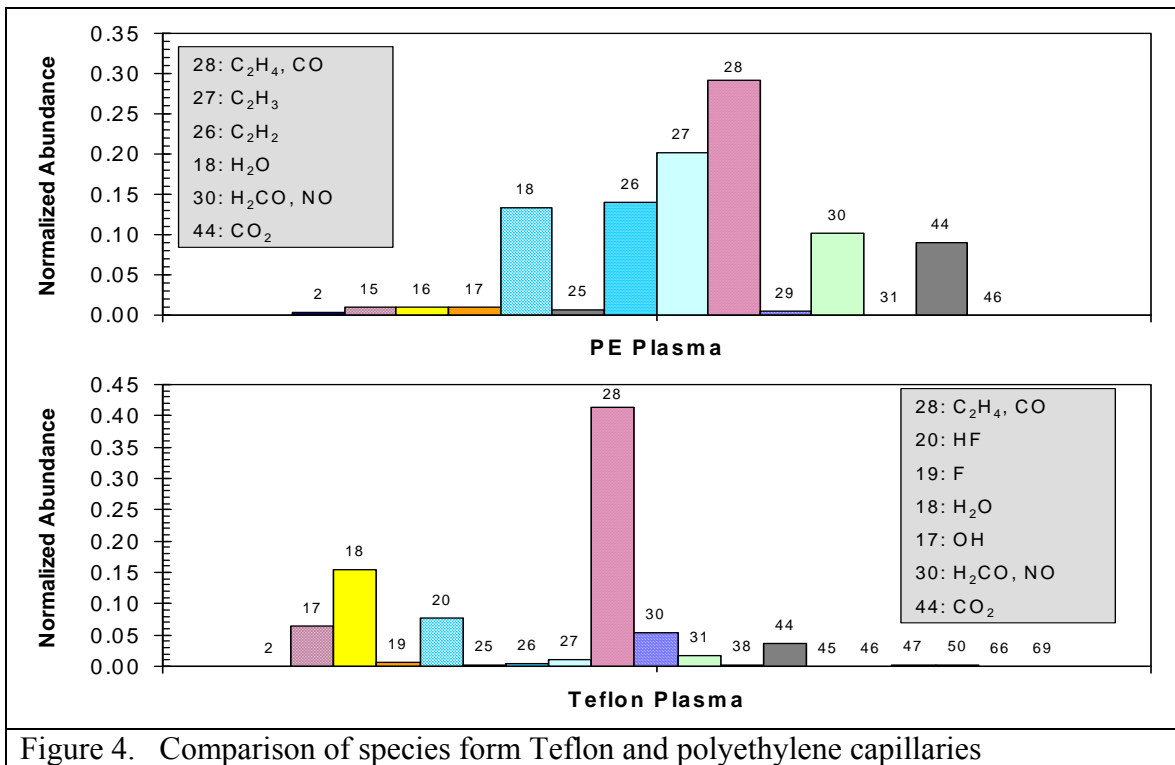


Figure 4. Comparison of species from Teflon and polyethylene capillaries

Species from Plasma-Propellant Interactions

Studies were conducted to investigate the details of the effects of plasma interaction with perforated JA-2 propellants samples that had been used in the mass loss testing conducted under a previous grant from ARO. Examination of the samples after impingement showed changes in color and surface morphology. The color change is from dark green to yellow green occurring in a layer from the exposed surface down to about 1–1.5 mm. Blisters are observed along the side surface of this layer. The plasma created a pitted area about 6–8 mm in diameter that was recessed about 0.5–1.0 mm from the original surface.

A detailed morphological analysis of this significantly modified surface was conducted using SEM coupled with x-ray detection for examination of any elemental variation. Figure 5 presents SEM microscopic images of the affected area with different magnifications; for comparison, an image of the virgin sample is also included in the figure. The SEM images show that, compared to the virgin sample, the exposed sample has dramatic changes in its surface morphology. Deformation of the perforations was found to be pronounced also. Evidences of melting, blisters as well as pits are evident on the surface at higher magnification.

As noted in the previous section, the plasma jet is composed of contributions from several sources, including the end electrode (anode), trigger wire, nozzle (cathode), capillary, and the air that is initially in the capillary. As a result, although by mole fraction the species from the hydrocarbon capillary dominate (about 90%) all other species, by mass fraction, it is the metals whose mass dominates the total mass of the

plasma jet. Therefore, it is not surprising that there are metallic particles present on the sample surface. The SEM images also show a broad size range of these particles, from one-tenth of a micron up to 50 microns.

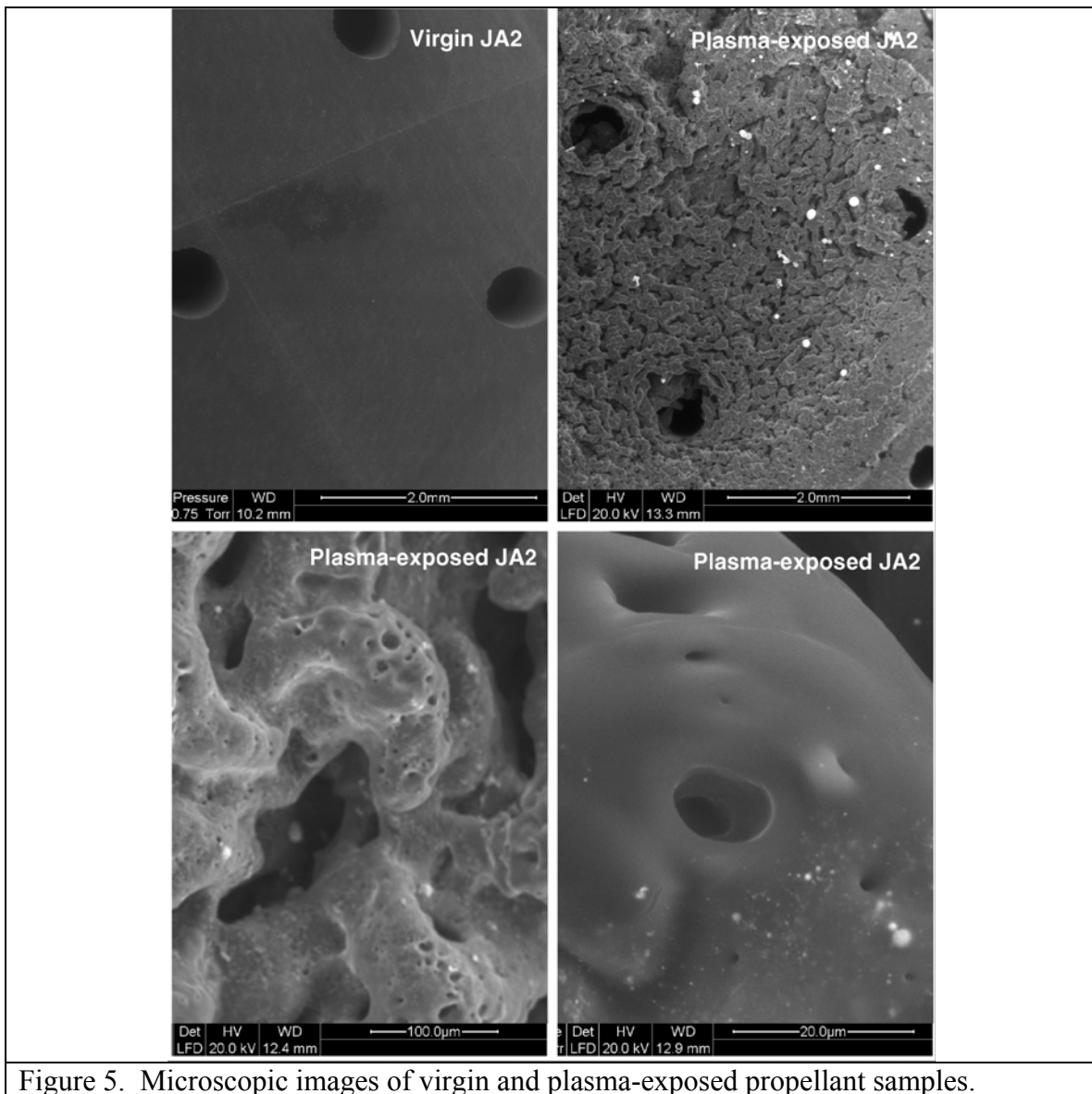
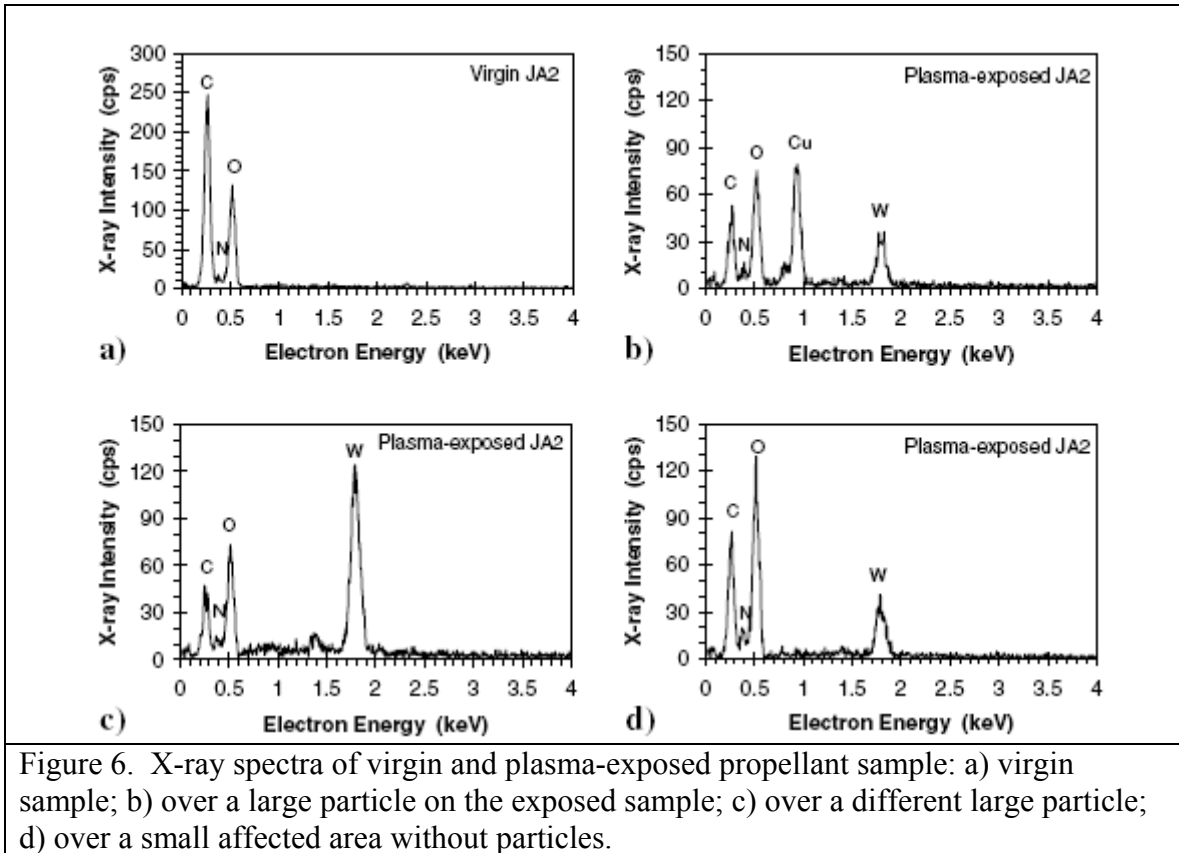


Figure 5. Microscopic images of virgin and plasma-exposed propellant samples.

These particles and their surrounding area were examined using an x-ray detector, the EDS, to identify the elemental compositions involved, and the results are shown in Figure 6. The spectrum of a virgin JA2 sample (Fig. 6a) shows the relative intensities of the elements contained in the propellant. The lack of hydrogen (H) in the spectrum is due to the fact that the smallest atomic element that the EDS can detect is carbon (C). The results for the exposed JA2 sample are given in Figs. 6b and 6c, where the spectra were obtained from scanning over two large particles and a small circular region surrounding the particle. It was found that one particle contains copper (Cu) and tungsten (W), while the other only tungsten. It is noted that particles that contain only copper were also

detected. The elements of carbon, nitrogen (N), and oxygen (O) are from the surrounding area. Figure 6d shows the spectrum scanning over a small area within which no clear evidence of particles is seen on the surface; however, tungsten can still be detected. This may suggest possible penetration of particles into the sample given the fact that in-depth detection of the x ray can be a few microns. It is also possible that a very thin film of the metal particles is formed on this area of the surface by a process similar to chemical vapor deposition.



Another interesting finding is that, compared to the spectrum of the virgin JA2, the spectra of the exposed sample seem to suggest that the sample has lost some carbon, because the intensity of carbon was significantly decreased. This result seems to suggest that species containing carbon may be the major decomposed products leaving the propellant sample during the plasma interaction.

These observed surface phenomena are a strong indicator that in-depth heating causes decomposition of the propellant. Some of the gaseous decomposition products accumulated in bubbles that burst, leaving pits in the surface; others remained trapped inside the propellant resulting in internal bubbles and/or blisters. The surface modification also suggests erosive ablation of surface material due to intense heating and dynamic interaction by the plasma jet. This intense heating primarily results from radiative and convective heat transfer as well as from shock impingement heating. In-depth gasification and surface ablation result in mass loss of the propellant sample.

Radiative Heat Transfer Measurements from Plasma

This part of the project was focused on measurement of the transient radiative flux and its interaction with a solid propellant. Additionally, for a better understanding on the role of thermal radiation during ETC ignition, the species evolved from radiative heating were collected and analyzed. In the early part of the project, a thin film heat flux gage was successfully developed, and coupled with the use of an inverse data reduction scheme, the transient variation of the radiant flux was deduced. Initial success of this thin film heat flux gage prompted its further development to allow measurement of much higher heat flux levels. However, the inverse data reduction scheme required an extension to heat conduction in two dimensions. The thin film heat flux gage was utilized in numerous material dependence and parametric studies. Finally, transparent and black JA2 samples were exposed to ETC radiation, and gas phase species produced from these propellant samples were analyzed using FTIR spectroscopy, and time-of-flight (ToF) mass spectrometry.

In these experimental studies, an ETC plasma was generated by exploding a thin metallic trigger wire, placed within a hydrocarbon capillary. A pulse-forming-network (PFN) circuit supplies the required electrical energy to explode the wire. Once evolved, the plasma sustains itself by ablating the hydrocarbon capillary, and emerges in an open-air environment as an underexpanded supersonic jet. The plasma jet then impinges over a stagnation plate that holds the heat flux and pressure gages. A Cordin high-speed CCD camera captures the relevant dynamics of the plasma jet. Additionally, current transducers are utilized to measure the current and voltage across the capillary. During these studies three different capillary and exploding wire materials were used: polyethylene (PE), lexan (LE), and Teflon (TE) as capillaries with copper (Cu), aluminum (Al), and nickel (Ni) as wires. Length and diameter of the capillary were 26mm, and 3mm respectively. For most of the experiments, trigger wire mass was 3.6mg. Nozzle exit to stagnation plate distance was varied between 5 to 75mm, and the plasma charging voltage varied between 2.5 to 7.5kV. The experiments utilized two PFN circuits with different capacitors (192 μ F and 865 μ F). Other important components of the PFN circuit comprise a 20 μ H inductor, a floating high-voltage mercury switch as ignitron, as well as an electrical circuit for charging the capacitor, and triggering the ignitron. As the PFN circuit is a slightly under-damped RLC circuit, a crowbar diode is utilized to prohibit the reverse flow of current through the capacitor. The trigger wire and the plasma act as the electrical resistance of the RLC circuit. A high-resistance bypass is also introduced for extra safety as well as voltage measurement across the capillary. Figure 7 shows the PFN circuit, plasma chamber and the stagnation plate location.

During this project, considerable efforts were expended for the design and manufacturing a reliable heat flux gage that can be utilized in a highly transient and electrically noisy environment. Initially a thin film gage was developed by sputtering 80 nm platinum over a polyimide substrate. Figure 8 shows the layer design of the gage as well as the LM134 constant current electrical circuit attached to it. For high heat flux measurements, the design was improved by replacing the polyimide substrate with sapphire. For both the cases, a fused silica window (transparent between 170-3000nm wavelength range) blocks the convective flux to reach the heat flux gages.

Typical current-voltage transience across the PE capillary, during the explosion of a 3.6mg Cu wire, is shown in Fig. 9. The charging voltage was varied from 2.5kV (0.90kJ) to 4.0kV (1.56kJ). Figure 10 shows the transient variation in stagnation pressure, radiant flux, and the gage temperature for 2.5kV plasma charging voltage, and 50mm distance from the plasma exit port to the stagnation plate. The voltage shows a quasi-steady behavior after the initial sharp peak, indicating the trigger wire explosion. The quasi-steady nature of the corresponding plasma jet, implying clear structures of an underexpanded jet, is shown in Fig. 11. The pressure peak shows the arrival of precursor shock at the stagnation plate. Radiant heat flux reaches its peak value simultaneously as the current peak, preceding the pressure peak. It is also observed that a faster plasma formation can be achieved by increasing the charging voltage. The studies also show that multistage radiative heating occurs when the plasma jet is allowed to travel larger distance. The gage design, experimental detail, as well as the radiant heat flux estimation procedure are discussed elsewhere in detail.¹¹

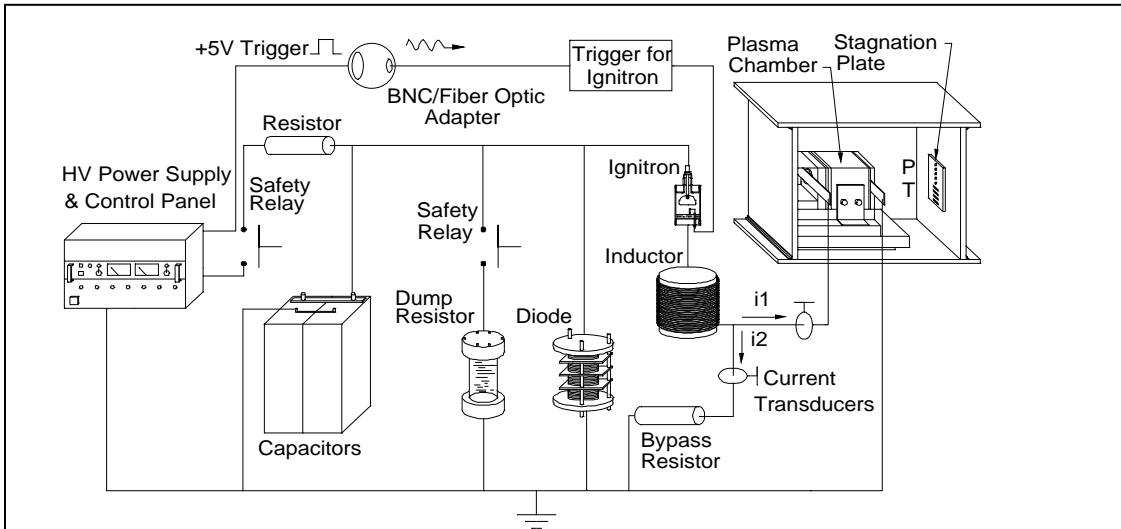


Fig. 7. Schematic of PFN circuit, plasma chamber, and location of stagnation plate.

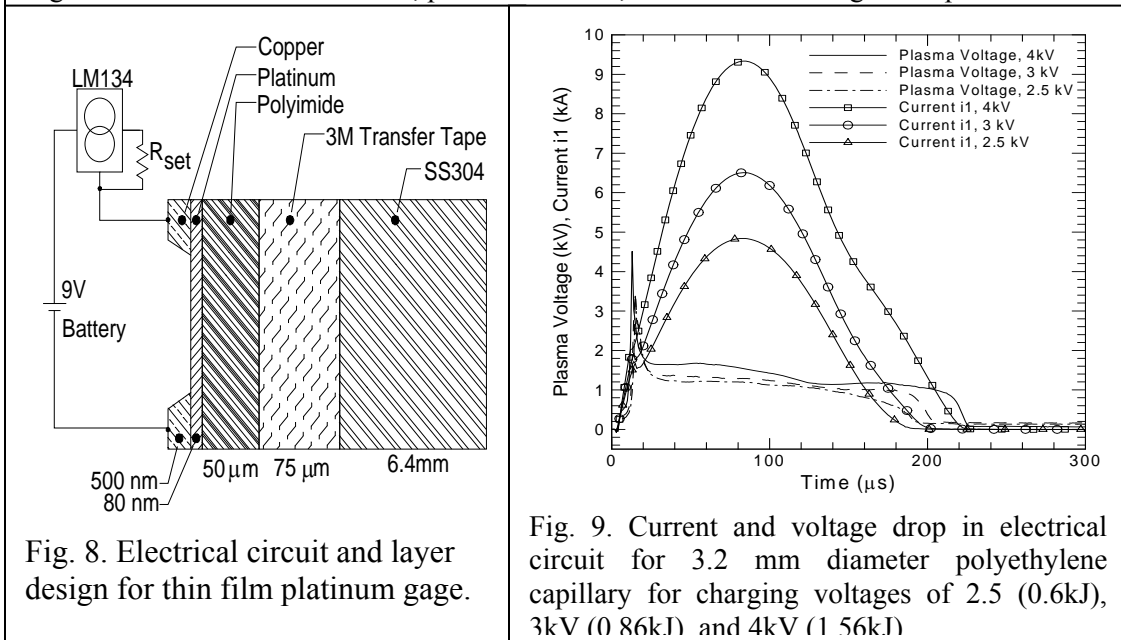


Fig. 8. Electrical circuit and layer design for thin film platinum gage.

Fig. 9. Current and voltage drop in electrical circuit for 3.2 mm diameter polyethylene capillary for charging voltages of 2.5 (0.6kJ), 3kV (0.86kJ) and 4kV (1.56kJ)

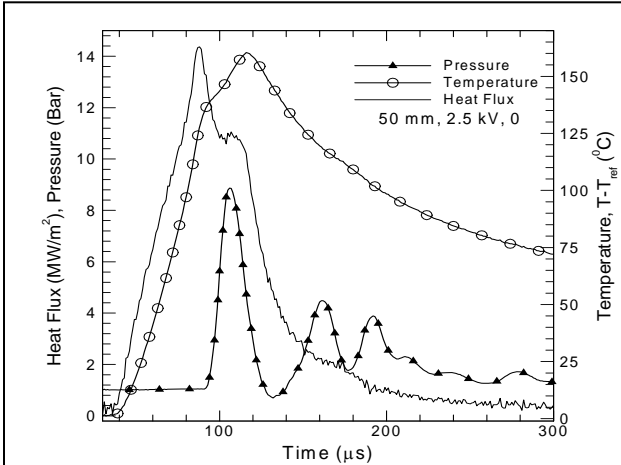


Fig. 10. Pressure, temperature, and radiant flux at the stagnation location for 2.5kV (0.90kJ) plasma; stagnation plate to plasma exit port distance = 50mm

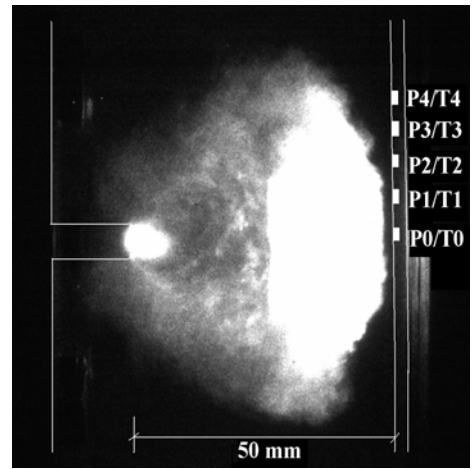


Fig. 11. Side view image of plasma jet for 2.5kV (0.90kJ) charging voltage.

With the initial success of the radiant flux, and stagnation pressure measurement, a material dependence study was undertaken. Three different capillary materials, namely, polyethylene, Lexan, and Teflon were combined with three trigger wire materials, copper, aluminum, and nickel. For all the experiments, following parameters were kept constant: charging voltage 2.5kV (0.90kJ), plasma exit port to stagnation plate distance 50mm, and trigger wire mass 3.6mg. Electrical current and voltage, radiant heat flux, as well as the stagnation pressure were measured. Figure 12 shows the transient variation in electrical current and voltage for all capillary and wire material combinations. Figure 13 shows the transient variation in the radiant flux, stagnation pressure, and the temperature rise of the heat flux gage. Table 2 show the corresponding ablation loss measured by a sensitive balance. Results reveal substantial differences in all measured parameters depending on the capillary, and trigger wire materials. It is found that higher material ablation leads to higher stagnation pressure, and lower radiant heat flux. LE-Al combination yielded maximum peak heat flux, whereas TE-Ni combination produced maximum peak value of stagnation pressure. Duration of the plasma initiation and formation process is also found to be material dependent. Detailed discussion of the material dependence studies are reported elsewhere.¹²

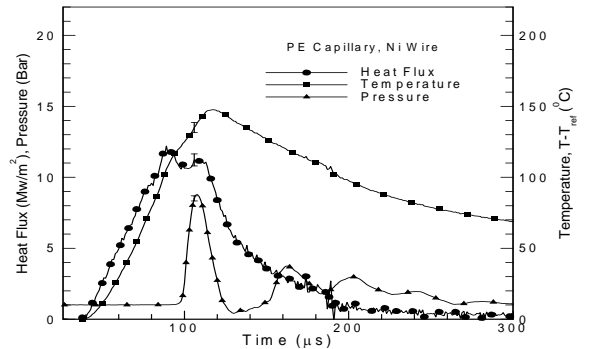
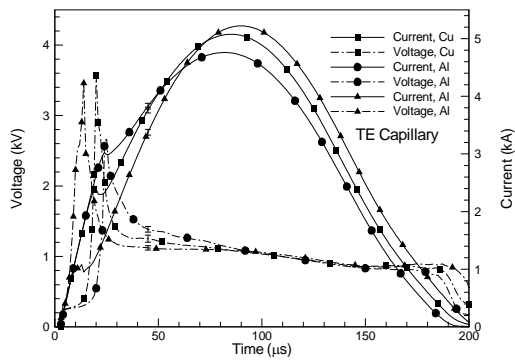
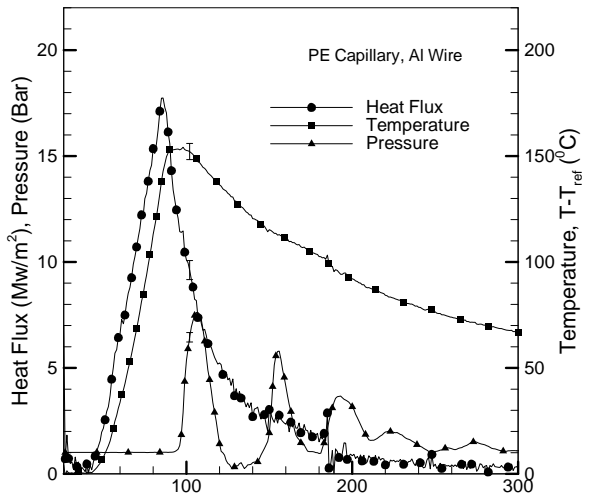
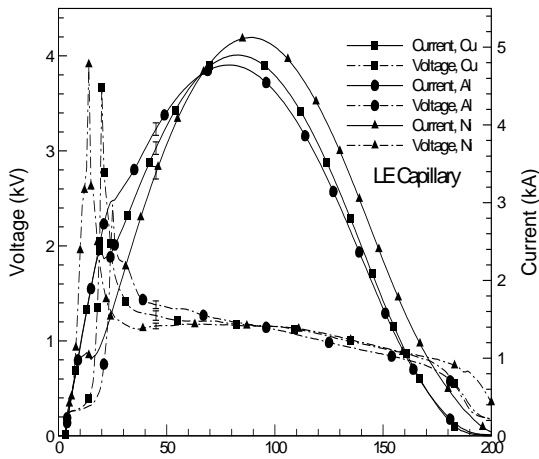
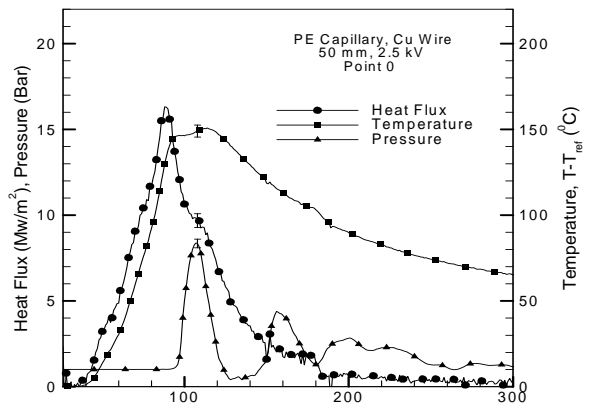
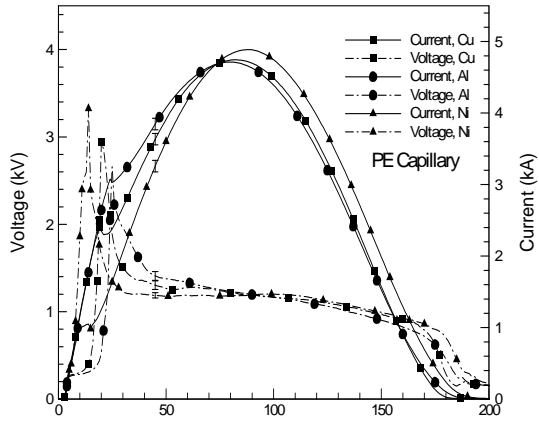


Fig. 12. Electrical current and voltage across capillary for different capillary and wire materials; charging voltage 2.5kV (0.90kJ)

Fig. 13. Transient pressure, temperature, and heat flux at the stagnation location (50 mm from plasma exit port) for PE capillary; charging voltage 2.5kV (0.90kJ)

Table 2. Mass ablated as well as average voltage and current for different capillary and wire material combinations.

Material	Ablated mass (mg)	Capillary (%)	Nozzle (%)	Electrode (%)	Wire (%)	V_{ave} (kV)	I_{ave} (kA)
PE+Cu	6.93	26.44	15.53	6.10	51.93	1.007	2.609
PE+Al	6.57	17.26	20.66	7.25	54.13	0.984	2.649
PE+Ni	6.19	26.39	11.68	3.76	58.17	1.070	2.632
LE+Cu	6.95	40.26	5.42	2.55	51.77	1.000	2.719
LE+Al	7.15	32.60	8.43	9.03	50.33	0.961	2.715
LE+Ni	6.52	38.34	2.04	4.41	55.21	1.076	2.832
TE+Cu	10.83	56.31	7.89	2.57	33.23	0.990	2.922
TE+Al	10.20	54.24	6.44	4.03	35.29	0.970	2.778
TE+Ni	11.23	57.86	8.31	1.78	32.05	1.054	2.949

Previous study showed that the platinum on polyimide heat flux gage was destroyed even for moderate energy level plasmas [11]. After careful examination of the material thermophysical properties, the platinum thin film was sputtered over sapphire instead of polyimide. It was observed that the newly designed heat flux gage successfully measures large radiant fluxes. The new gage, however, due to larger thermal penetration depth, requires a multidimensional algorithm for radiant heat flux calculation. A two-dimensional inverse scheme was formulated to address this issue. The algorithm was developed around conjugate-gradient optimization technique with iterative regularization. Two-dimensional effects were quantified and the general criteria for identifying multidimensional effects in heat flux gages were established. Figure 14 shows the performance of one- and two-dimensional (1-D and 2-D) algorithms in estimating radiant flux from a 7.5kV (5.4kJ) plasma jet. The plasma was generated in a 3mm diameter, 26mm long polyethylene capillary, by exploding 3.6mg copper trigger wire. Plasma exit port to stagnation plate distance was fixed at 50mm. The figure shows substantial mismatch between the two formulations. Table 3 shows the two-dimensional effects for different plasma energy levels. Two-dimensional effect was quantified by defining a relative error term e :

$$e = \left| \frac{q''(2-D) - q''(1-D)}{q''(2-D)} \right| \times 100\% \quad (1)$$

where q'' is the calculated radiant heat flux from inverse algorithm. Investigation revealed that the Fourier number, based on gage width, is an important parameter for calculating 2-D effect, and that the 2-D effect is largely independent of the nature of the heat flux

profile. Further discussion of the inverse formulation and computation detail are reported elsewhere.¹³

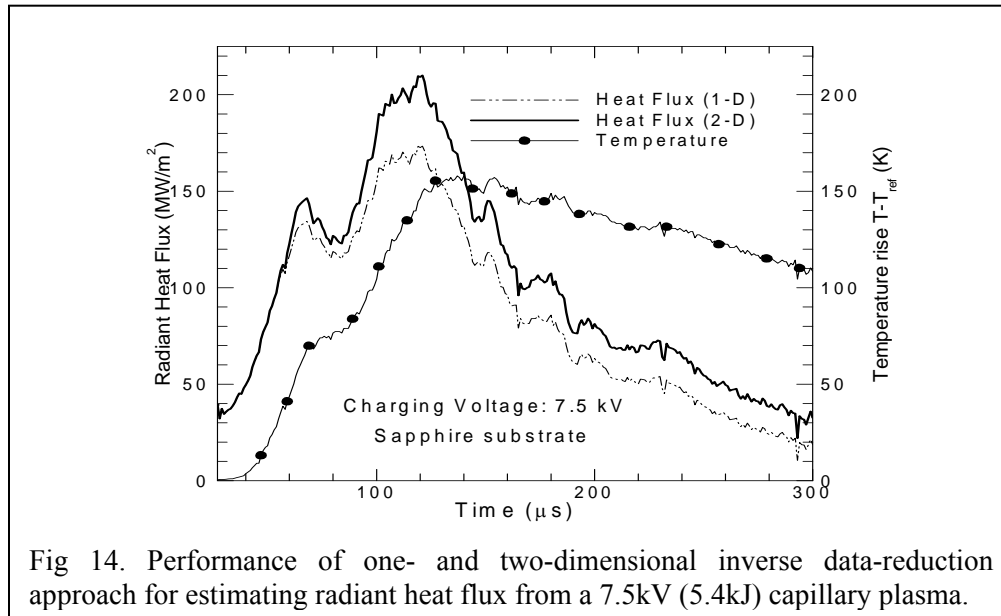


Fig 14. Performance of one- and two-dimensional inverse data-reduction approach for estimating radiant heat flux from a 7.5kV (5.4kJ) capillary plasma.

Table 3. Relative difference between the 1-D and 2-D algorithms in estimated heat fluxes for different charging voltages and substrate material.

Charging Voltage (kV)	Substrate material	e at peak heat flux location (%)	e averaged over 0 to 500 μ s, e_{av} , (%)
2.5	Polyimide	5.23	7.65
4.0	Sapphire	22.60	33.24
5.0	Sapphire	19.14	31.11
7.5	Sapphire	17.47	21.02

Radiative Ignition of Double-Base Propellants

After the gage design and the data reduction techniques were standardized, further studies were undertaken to investigate the role of radiative heating in ETC ignition of transparent and black JA2 propellants. Both of these propellants are double-base nitroesters containing 14.9% nitroglycerine (NG), 59.5% nitrocellulose (NC), and 24.8% diethylene glycol dinitrite (DEGDN). Additionally, black JA2 contains 0.05% of carbon, while the transparent JA2 is carbon-free. JA2 samples (~75mg) were placed in an ignition chamber and exposed to ETC plasma radiation. Results reveal that due to difference in radiative properties, transparent JA2 allows radiative flux to travel deep below the exposed surface, generating void structures that are absent in unexposed samples. Black JA2, being opaque, absorbs most of the radiation on its surface, and thus produces greater mass loss with noticeable change in surface color. Additionally, during the ETC exposure of the propellants, the pressure rise within the ignition chamber is measured as well as the

generated gas is collected within a collection chamber, maintained in an inert (helium-argon) atmosphere. The solid propellants as well as the collected gas samples were analyzed using FTIR spectroscopy and ToF mass spectrometry. The experiments were conducted up to 30kJ of plasma energy level. It is, however, observed that the propellant samples never reach ignition and steady-state combustion. Figure 15 shows the pressure rise within the ignition chamber, and the propellant mass loss, when black JA2 samples are exposed to ETC radiation of varying energy levels. Figure 16 shows that transparent JA2 samples (0.50mg), when undergoes rapid thermal decomposition, produces substantial amount of NO_2 .

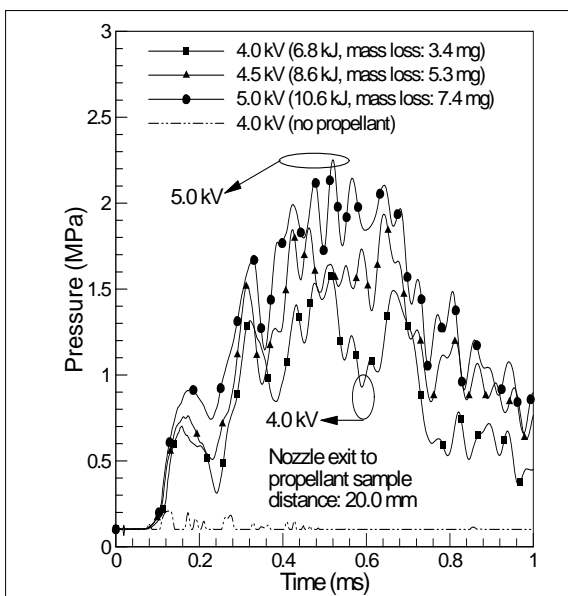


Fig. 15. Chamber pressure variation during confined radiative pyrolysis of black JA2.

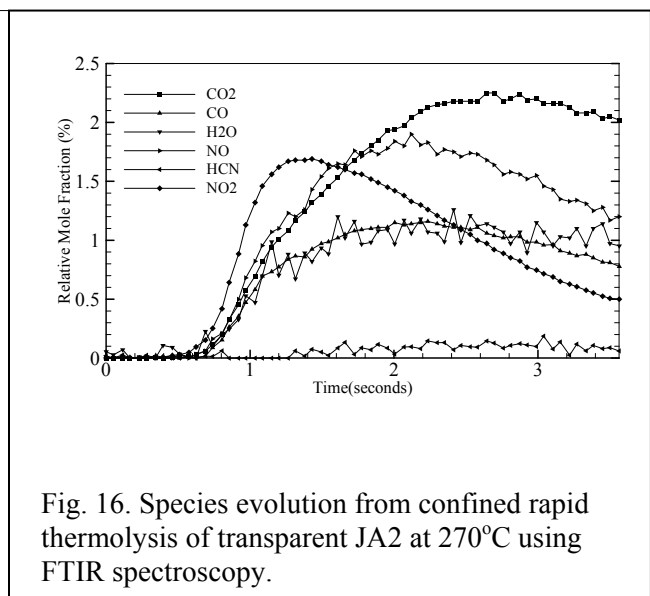
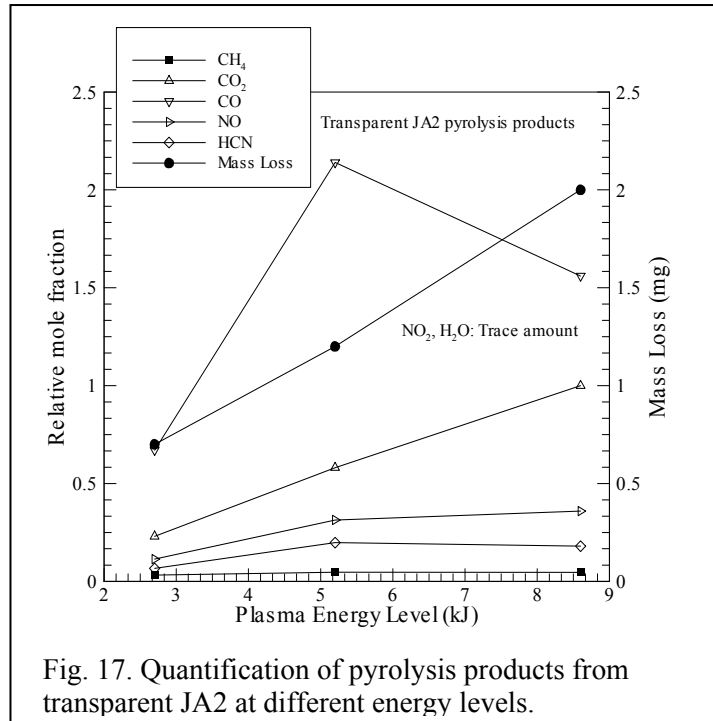


Fig. 16. Species evolution from confined rapid thermolysis of transparent JA2 at 270°C using FTIR spectroscopy.

Figure 17 shows the gas phase species generated during ETC radiation exposure of the transparent JA2 propellants. Results reveal absence of NO_2 and H_2CO in the gas phase species irrespective of plasma energy level. During nitroester decomposition, NO_2 , produced during the primary reversible homolysis reaction, acts as an autocatalytic agent that accelerates the initial decomposition reactions leading to ignition, and consequent steady-state combustion of the propellant. Additionally, it is well known that UV exposure of NO_2 results in UV-photolysis that breaks down the NO_2 to NO and O_2 . UV radiation, therefore, prohibits nitroester propellant ignition through UV photolysis. ETC plasma, due to its high temperature ($\sim 25,000\text{K}$), generates substantial UV radiation. It is, therefore, quite likely that in a moderate energy ETC gun, radiation alone will not be able to ignite the propellant. Further details of the UV-photolysis, radiative pyrolysis, and rapid thermal decomposition of JA2 are discussed elsewhere.¹⁴ Additional work is currently underway and will be presented at the next JANNAF meeting.



TECHNOLOGY TRANSFER

Throughout the project, the investigators made several trips to ARL at Aberdeen Proving Ground and made presentations on our progress. We are grateful for the feedback from Drs. M. Nusca, R. Pesce-Rodriguez and R. Beyer. Dr. K. McNesby also received samples of our heat flux gages. Additionally, Dr. Beyer of ARL has kindly furnished additional components to the electrical discharge circuit. Propellant samples were shipped to us by Drs. J. Yu and S. Ritchie of ATK.

REFERENCES

- ¹ Beyer, R. A., and Pesce-Rodriguez, R. A., "Experiments to Define Plasma-Propellant Interactions," *IEEE Transactions on Magnetics*, Vol. 39, No. 1, 2003, pp. 207-211.
- ² Fifer, R. A., Sagan, E. S., and Beyer, R. A., "Chemical Effects in Plasma Ignition," *IEEE Transactions on Magnetics*, Vol. 39, No. 1, 2003, pp. 218-222.
- ³ Perelmutter, L., Sudai, M., Goldenberg, C., Kimhe, D., Zeevi, Z., Arie, S., Melnik, M., and Melnik, D., "Temperature Compensation by Controlled Ignition Power in SPETC Guns," *Proceedings of the 16th International Symposium on Ballistics*, San Francisco, 1996, pp. 145-152.
- ⁴ Birk, A., Del Guercio, M., Kinkennon, A., Kooker, D. E., and Kaste, P., "Interrupted-Burning Tests of Plasma Ignited JA2 and M30 Grains in a Closed Chamber," *Propellants, Explosives, Pyrotechnics*, Vol. 25, No. 3, 2000, pp. 133-142.

- ⁵ Kim, J. U., Clemens, N. T., and Varghese, P. L., “Experimental Study of the Transient Underexpanded Jet Generated by Electrothermal Capillary Plasma,” *Journal of Propulsion and Power*, Vol. 18, No. 6, 2002, pp. 1153-1160.
- ⁶ Kappen, K., and Beyer, R. A., “Progress in Understanding Plasma-Propellant Interaction,” *Propellants, Explosives, Pyrotechnics*, Vol. 28, No. 1, 2003, pp. 32-36.
- ⁷ Li, J.-Q., Litzinger T. A., and Thynell, S. T., “Interactions of Capillary Plasma with Double-base and Composite Propellants,” *Journal of Propulsion and Power*, Vol. 20, No. 4, 2004, pp. 675-683.
- ⁸ Li, J.-Q., Litzinger, T. A., and Thynell, S. T., “Plasma Ignition and Combustion of JA2 Propellant,” *Journal of Propulsion and Power*, Vol. 21, No. 1, 2005, pp. 44-53.
- ⁹ Kohel, James M.; Su, Lester K.; Clemens, Noel T.; Varghese, Philip L., Emission spectroscopic measurements and analysis of a pulsed plasma jet, *IEEE Transactions on Magnetics*, v 35, n 1 pt 1, Jan, 1999, p 201-204
- ¹⁰ Li, Jianquan; Litzinger, Thomas A.; Das, Malay; Thynell, Stefan T., Recombination of electrothermal plasma and decomposition of plasma-exposed propellants, *Journal of Propulsion and Power*, v 22, n 6, 2006, p 1353-1361.
- ¹¹ Das, M., Thynell, S. T., Li, J.-Q., and Litzinger, T., “Transient radiative Heat Transfer From a Plasma Produced by a Capillary Discharge”, *Journal of Thermophysics and Heat Transfer*, Vol. 19, No. 4, 2005, pp. 572-580.
- ¹² Das, M., Thynell, S. T., Li, J.-Q., and Litzinger, T., “Material Dependence of Plasma Radiation Produced by a Capillary Discharge”, *Journal of Thermophysics and Heat Transfer*, Vol. 20, No. 3, 2006, pp. 595-603.
- ¹³ Das, M., and Thynell, S. T., “Two-dimensional Conduction Effects in Estimating Radiative Flux from a Capillary Discharge”, *Journal of Thermophysics and Heat Transfer*, Vol. 20, No. 4, 2006, pp. 903-911.
- ¹⁴ Das, M. K., Chowdhury, A., and Thynell, S. T., “Radiative Pyrolysis of JA2 from an Electrochemical Plasma Discharge”, *Proceedings of the Eastern States Section of the Combustion Institute*, University of Virginia, Oct 21-24, 2007.